A Density Distance Augmented Chan-Vese Active Contour for CT Bone Segmentation

Phan T. H. Truc, Sungyoung Lee, and Tae-Seong Kim, *Member, IEEE*

Abstract— Bone segmentation from Computed Tomography (CT) images is a critical component in computer-assisted orthopedic surgery but is a challenging task. Among many active contour (AC) models employed to solve the problem, the Chan-Vese AC [1] yields superior performances as evaluated in [2]. However, the CV AC fails to correctly extract the objects that are of high inhomogeneity because its nature is the minimization of the differences within the objects. In this paper, we propose to incorporate a Bhattacharrya term to the CV functional which helps to maximize the distance between the density functions of the objects and the background. The proposed model is tested with various synthetic and real CT images. Preliminary experimental results show that it can overcome the limitation of the CV AC.

I. INTRODUCTION

Bone segmentation from Computed Tomography (CT) images is a critical component in computer-assisted orthopedic surgery but is a challenging task due to inhomogeneous bone structures, low contrast edges, and overlapping intensity values of bones [3]. As surveyed in [4], although there are many attempts on this problem, none of them claims fully satisfactory performance. On the other hand, since it was first introduced in [5], active contour (AC) has attracted a large amount of researches and become one of the most widely used techniques in image segmentation. Many of AC models have also been developed for CT bone segmentation [6], [3], [7]. Particularly, the authors in [2] have evaluated different AC models and shown that the Chan-Vese (CV) AC [1], [8] provides superior performances among them for the considered data set in terms of accuracy and user-interaction.

However, the convergence of the CV AC depends on the homogeneity of the segmented objects. When the inhomogeneity becomes so large like in some carpal bones or knee bones, the CV AC provides unsatisfactory results. One possible reason is that the global minima do not always guarantee the "desirable" segmentation result. Consider a simple example of a phantom image with four different objects as shown in Fig. 1. The image intensity is scaled on the range $[0, 1]$, with 1 the brightest. The CV AC is used to segment the objects. At each iteration during its evolution, we calculate the CV "fitting term", $F(C)$, using (1) in Section II and plot it in Fig. 2. As expected, the curve moves in the direction of decreasing $F(C)$ and stops when $F(C)$ reaches a minimum value, which is $F(C^*) = 202$ (at iteration number 35) in
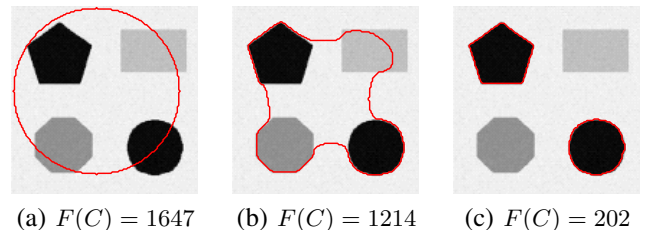
P. T. H. Truc and S. Y. Lee are with the Department of Computer Engineering, Kyung Hee University, Rep. of Korea, 446-701.

T.-S. Kim is with the Department of Biomedical Engineering, Kyung Hee University, Rep. of Korea, 446-701. tskim@khu.ac.kr.

(a) $F(C) = 1647$ (b) $F(C) = 1214$ (c) $F(C) = 202$

Fig. 1. An example of a phantom image (size 130×130) where the CV AC (in red color) fails. Only two out of four objects are segmented. (a) Initial, (b) Intermediate, and (c) Final curve. The plot of $F(C)$ at every iteration is given in Fig. 2.
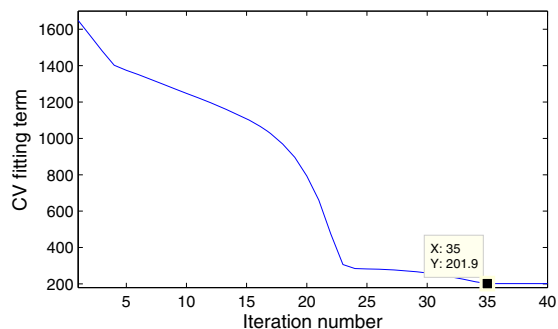

Fig. 2. CV fitting term $F(C)$ at every iteration of the CV AC evolution process. The obtained minimum (≈ 202) is not the "desirable" one (≈ 555).

this case. Nevertheless, this is not the satisfactory result since only two out of four objects are segmented. When manually placing the curve on the desired position (capturing all four objects), we obtain the "desirable" minimum as $F(C^{des}) = 555$. Clearly, the desirable minimum here is larger (more local) than the practically resulting minimum $F(C^*)$.

The unsatisfactory result of the CV AC in this case is due to the fact that it is trying to minimize the dissimilarity within each segment but does not care about the distance between different segments. In this paper, we propose to incorporate an evolving term based on the Bhattacharyya distance [9] to the CV fitting term. This new term helps to maximize the distance between density functions of the objects and the background. As a result, by changing a weighting parameter, the new flow can flexibly drive the AC towards the desirable minimum.

The rest of the paper are organized as follows. Section II describes the proposed approach in details. Then, experimental results are shown in Section III. Finally, the paper is concluded in Section IV.

II. METHODOLOGY

A. The Proposed Model

Let $\mathbf{x} \in \mathbb{R}^2$ be the coordinates of a pixel in the image plane $\Omega \subset \mathbb{R}^2$. Let $I : \Omega \to \mathcal{Z}$ be a mapping from the image plane to the space of a certain image feature such as intensity, a color vector, a texture vector, or a vector of geometric measures (e.g., structure tensors), etc.

The Chan-Vese model [1] is $\inf_C F(C)$, where

$$F(C) = \int_{inside(C)} |I(\mathbf{x}) - c_{in}|^2 \, d\mathbf{x} \qquad (1)$$
$$+ \int_{outside(C)} |I(\mathbf{x}) - c_{out}|^2 \, d\mathbf{x},$$

with c_{in} and c_{out} respectively the mean values of image features inside and outside the curve C, which partitions the image into two regions corresponding to object(s) and background. This model searches for a curve position that minimizes the differences of image features within each region. Compared to other AC models, it has many advantages such as ability to detect objects with very smooth edges, robustness to noise, and less sensitivity to initialization. However, it fails to capture objects with high inhomogeneity like bones in CT images.

We propose to incorporate a global term $B(C)$ which is based on the Bhattacharrya distance between the density functions inside and outside C: $p_{in}(z)$ and $p_{out}(z)$, $z \in \mathcal{Z}$ as follows:

$$E_0(C) = \beta F(C) + (1 - \beta)B(C) \qquad (2)$$

where $B \equiv B(C) = \int_{\mathcal{Z}} \sqrt{p_{in}(z)p_{out}(z)}dz$ is the Bhattacharyya coefficient [9] and $\beta \in [0,1]$ a constant that balances the contributions of the two terms. Note that the Bhattacharyya distance is defined by $[-\log B(C)]$ and the maximization of this distance is equivalent to the minimization of $B(C)$. As normal, we can regularize the solution by constraining the length of the curve and the area of the region inside it. Therefore, the energy functional is defined by

$$E(C) = \gamma Length(C) + \eta Area(inside(C)) \qquad (3)$$
$$+ \beta F(C) + (1 - \beta)B(C).$$

The intuition behind the proposed energy function is that we seek for a curve that:

1) is regular, of minimal length and area (the first two terms) and
2) partitions the image into two regions such that the differences within each region are minimized (the $F(C)$ term) and the Bhattacharyya distance between the two regions is maximized (the $B(C)$ term).

For the level set formulation, we use the Heaviside function $H(\cdot)$ and the Dirac function $\delta_0(\cdot)$ defined by

$$H(u) = \begin{cases} 1, & \text{if } u \geq 0 \\ 0, & \text{if } u < 0, \end{cases} \qquad \delta_0(u) = \frac{d}{du}H(u)$$

and represent the curve C by the zero level set of a Lipschitz function $\phi : \Omega \to \mathbb{R}$ such that

$$\begin{cases} C & = \{\mathbf{x} \in \Omega : \phi(\mathbf{x}) = 0\}, \\ inside(C) & = \{\mathbf{x} \in \Omega : \phi(\mathbf{x}) < 0\}, \\ outside(C) & = \{\mathbf{x} \in \Omega : \phi(\mathbf{x}) > 0\}. \end{cases}$$

Then, the energy functional can be rewritten as

$$E(C) = \gamma \int_\Omega |\nabla H(\phi(\mathbf{x}))|d\mathbf{x} + \eta \int_\Omega H(-\phi(\mathbf{x}))d\mathbf{x}$$
$$+ \beta \left[\int_\Omega |I(\mathbf{x}) - c_{in}|^2 H(-\phi(\mathbf{x}))d\mathbf{x} + \right.$$
$$\left. \int_\Omega |I(\mathbf{x}) - c_{out}|^2 H(\phi(\mathbf{x}))d\mathbf{x} \right] \qquad (4)$$
$$+ (1 - \beta) \int_{\mathcal{Z}} \sqrt{p_{in}(z)p_{out}(z)}dz$$

where $\gamma \geq 0$, $\eta \geq 0$ are fixed parameters, and

$$p_{in}(z) = \frac{\int_\Omega \delta_0(z - I(\mathbf{x}))H(-\phi(\mathbf{x}))d\mathbf{x}}{\int_\Omega H(-\phi(\mathbf{x}))d\mathbf{x}},$$
$$p_{out}(z) = \frac{\int_\Omega \delta_0(z - I(\mathbf{x}))H(\phi(\mathbf{x}))d\mathbf{x}}{\int_\Omega H(\phi(\mathbf{x}))d\mathbf{x}}. \qquad (5)$$

Considering slightly regularized versions of the functions H and δ_0, denoted here by H_ϵ and δ_ϵ as $\epsilon \to 0$ and using the calculus of variation and the gradient descent method, we can derive the evolution flow associated with minimizing the energy functional in (4) as

$$\frac{\partial \phi}{\partial t} = \delta_\epsilon(\phi)\left\{ \gamma\kappa + \eta + \beta \left[(I - c_{in})^2 - (I - c_{out})^2 \right] \right.$$
$$- (1 - \beta)\left[\frac{B}{2}\left(\frac{1}{A_{in}} - \frac{1}{A_{out}} \right) + \right.$$
$$\left. \left. \frac{1}{2}\int_{\mathcal{Z}}\delta(z - I)\left(\frac{1}{A_{out}}\sqrt{\frac{p_{in}}{p_{out}}} - \frac{1}{A_{in}}\sqrt{\frac{p_{out}}{p_{in}}} \right) dz \right] \right\} \qquad (6)$$

where A_{in} and A_{out} are respectively the areas inside and outside the curve C and are given by

$$A_{in} = \int_\Omega H(-\phi(\mathbf{x}))d\mathbf{x}, \quad A_{out} = \int_\Omega H(\phi(\mathbf{x}))d\mathbf{x}. \qquad (7)$$

B. Implementation

There are a couple of possible regularizations of function H (and δ_0) [1], [10] which determine the number of level curves that the evolution flow for ϕ acts on. Some regularizations make the flow acts on a few level curves around the zero level set $\{\phi(\mathbf{x}) = 0\}$ whilst some others acts on all level curves. In this paper, we choose to replace $\delta_0(\cdot)$ by $|\nabla\phi|$ to extend the evolution to all level sets of ϕ as suggested in [10] so that we can obtain a global minimizer.

The pseudo-code for the proposed algorithm can be outlined as follows:

- $k = 0$, initialize ϕ^k by ϕ_0.
- Compute the mean values c_{in} and c_{out}.
- Compute $p_{in}(z)$ and $p_{out}(z)$ according to (5).
- Compute A_{in} and A_{out} by (7).
- Evolve the curve using (6) to obtain ϕ^{k+1}.
- Reinitialize ϕ as the signed distance function of the current curve (see [11] for details).
- Check whether convergence is met. If not, $k = k+1$ and go back to the second step.

III. EXPERIMENTAL RESULTS

In this section, we test the proposed model on various synthetic and real images. The image feature employed is intensity. We choose a fixed setting as follows: $\gamma = 0.3$ and $\eta = 0$. The weighting parameter β is not same for all experiments and will be specified in each case. If the objects we want to segment are of high homogeneity, then β should be small and vice versa. The cpu time, in seconds, of our calculations performed on a Pentium IV Duo Core 1.87 GHz with 1GB of RAM will also be provided.

Let us get back to the phantom image in the example in Section I. The curve is initialized exactly same as in Fig. 1(a) and the evolving process is demonstrated in Fig. 3. It is possible to see that all four objects are detected, i.e., the "desirable" minimum of $F(C)$ is successfully found. The finding process is shown in Fig. 4 for a comparison against that in Fig. 2.

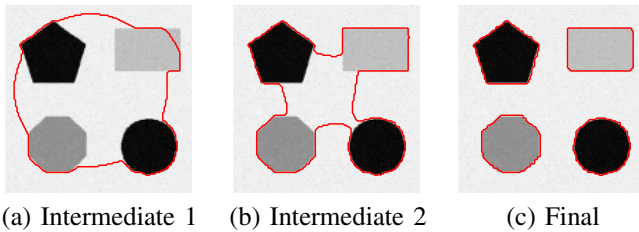(a) Intermediate 1   (b) Intermediate 2   (c) Final

Fig. 3. Result of the proposed model applied on the example image in Fig. 1 using the same initialization. All four objects are segmented correctly. $\beta = 0.5$ and cpu time = $66s$. The plot of $F(C)$ is given in Fig. 4.
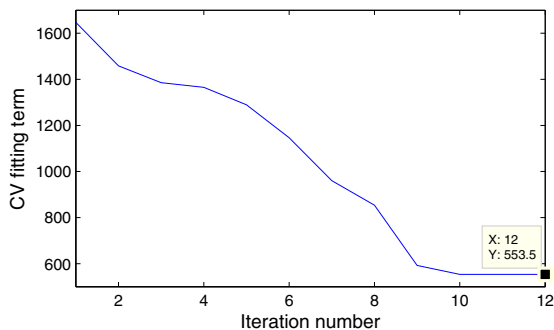

Fig. 4. CV fitting term $F(C)$ at every iteration of the proposed AC evolution process. The "desirable" minimum is found.

Fig. 5 shows how the proposed model works on a noisy synthetic image. The objects are of knee bone shape and are
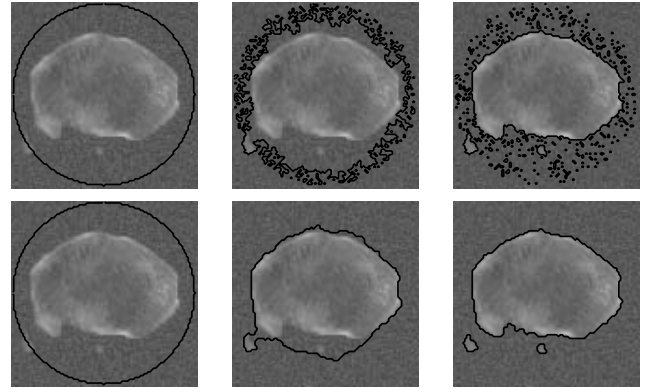

Fig. 5. Detection of bone-shape objects in noisy image, size = 100×100. Upper row: CV AC, cpu time = $62s$. Lower row: the proposed AC, $\beta = 0.3$ and cpu time = $46s$.

correctly extracted despite background noise. The CV AC, on the other hand, can detect the objects but captures some speckle noise also.

To show the effectiveness of our model in segmenting objects having low contrast, we create testing data as follows. First, a medical expert is asked to manually extract bone region in a real CT image. Then, we place the extracted bone on homogeneous backgrounds with various intensities such that the contrast of the image differs from 1% to 20%. Here we adopt the definition of contrast introduced by Morrow et al. [12]

$$contrast = \frac{M_0 - M}{M_0 + M}100\% \qquad (8)$$

where M and M_0 are respectively the mean intensity of the object (foreground) and the surrounding region (background) in an image. In our real CT image, the contrast is about 8%. To our knowledge, CT images with the contrast of 20% are quite clear and those with the contrast of 1% are beyond the worst case. By this way we can have testing images with typical CT bone segmentation challenges. The images are of size 100×100 and contain three separate bone segments (note that the small segment is also bone).

The obtained segmentation results are compared with the known "ground truth", and the *accuracy* measure, defined as the ratio between the number of pixels that are correctly classified (as bone and background) and the total number of pixels in the image, is used for quantitative evaluation. Fig. 6 show a sample result for a testing image having contrast of 1% while the *accuracy* values for the whole data set are plotted in Fig. 7. We can see that the proposed model yields higher accuracy than the CV AC does, especially at low contrast level.

Fig. 8 shows the segmentation results for a real CT image using CV AC and the proposed model. The image is of size 300×300 and belongs to the knee region of a patient. Again, it can be seen that the CV AC fails to capture the bone region while the proposed model can. The reason is that the soft tissue region (background) in this image is not homogeneous enough.
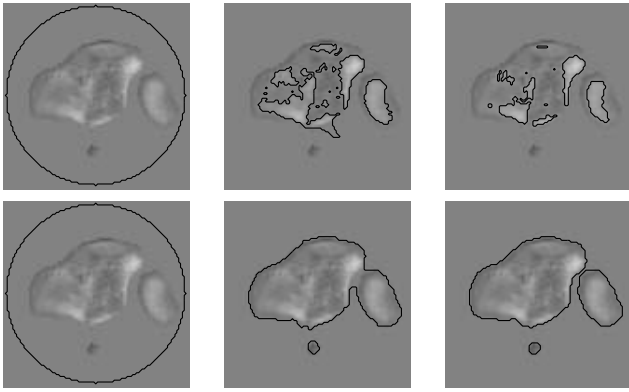
Fig. 6. Sample result for a testing image having contrast of 1%. Size = 100×100. Upper row: CV AC, cpu time = $58s$. Lower row: the proposed model, $\beta = 0.3$, cpu time = $64s$.
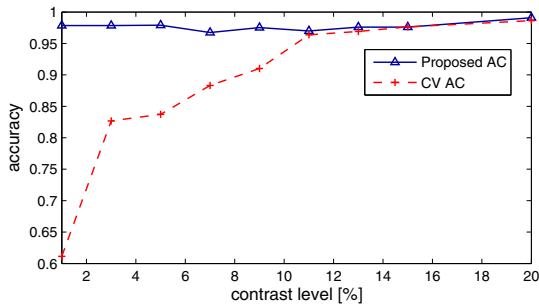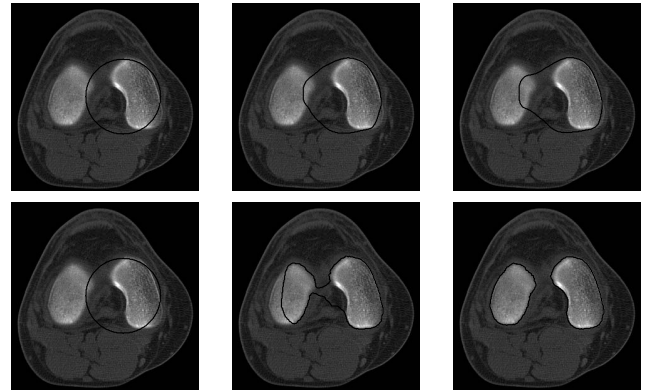

Fig. 8. Result for a real CT image of size 300×300. Upper row: CV AC, cpu time = $213s$. Lower row: the proposed model, $\beta = 0.5$, cpu time = $168s$.

Fig. 7. Plots of accuracy vs. contrast level. The proposed AC performs better than the CV AC, especially when the contrast is less than 9%.

IV. CONCLUSION AND FUTURE WORK

In this paper, we have proposed a novel AC model to extract bone regions from CT images. The proposed model incorporates to the CV energy functional the Bhattacharyya distance between the density functions inside and outside the curve to drive it towards a "desirable" minimum which is often not the global one. The evolution flow of the proposed model is derived using the level set framework, making it inherit advantages of a geometric AC such as topology adaptability. Experimental results show that the proposed AC overcomes the limitation of the CV AC when dealing with images having inhomogeneous objects with more robustness to contrast level. It is also possible to see that the cpu time of our model is comparable to or even less than that of the CV AC despite the higher computational cost. This is due to the fact that the additional evolving term helps to move the curve faster towards convergence. Qualitatively satisfactory results of the proposed model applied on a real CT image demonstrate its potential in medical image segmentation. Quantitative evaluation on large data sets of CT images will be done in our future work to quantify its effectiveness. Also, image features other than intensity may be considered.

REFERENCES

[1] T. Chan and L. Vese, "Active contours without edges," *IEEE Trans. Image Proc.*, vol. 10, pp. 266–277, 2001.

[2] P.-T.-H. Truc, T.-S. Kim, Y.-H. Kim, Y.-B. Ahn, Y.-K. Lee, and S.-Y. Lee, "Automatic bone segmentation from CT images using Chan-Vese multiphase active contour," *J. Biomed. Eng. Res.*, vol. 28, no. 6, pp. 713–720, Dec. 2007.

[3] T. Sebastian, H. Tek, J. Crisco, and B. Kimia, "Segmentation of carpal bones from CT images using skeletally coupled deformable models," *Medical Image Analysis*, vol. 7, pp. 21–45, 2003.

[4] L. Wang, M. Greenspan, and R. Ellis, "Validation of bone segmentation and improved 3-D registration using contour coherence in CT data," *IEEE Trans. Med. Imag.*, vol. 25, pp. 324–334, 2006.

[5] M. Kass, A. Witkin, and D. Terzopoulos, "Snakes: active contour models," *Int. J. Comput. Vis.*, vol. 1, no. 4, pp. 321–331, 1988.

[6] X. M. Pardo, M. J. Carreira, A. Mosquera, and D. Cabello, "A snake for CT image segmentation integrating region and edge information," *Image Vis. Comput.*, vol. 19, pp. 461–475, 2001.

[7] W. Yao, P. Abolmaesumi, M. Greenspan, and R. Ellis, "An estimation/correction algorithm for detecting bone edges in CT images," *IEEE Trans. Med. Imag.*, vol. 24, pp. 997–1010, 2005.

[8] L. Vese and T. Chan, "A multiphase level set framework for image segmentation using Mumford and Shah model," *Int. J. Comp. Vis.*, vol. 50, no. 3, pp. 271–293, 2002.

[9] T. Kailath, "The divergence and Bhattacharyya distance measures in signal selection," *IEEE Trans. Commun. Technol.*, vol. 15, pp. 52–60, Feb. 1967.

[10] H.-K. Zhao, T. Chan, B. Merriman, and S. Osher, "A variational level set approach to multiphase motion," *J. Comput. Phys.*, vol. 127, pp. 179–195, 1996.

[11] S. Osher and R. P. Fedkiw, *Level set methods and dynamic implicit surfaces.* New York, USA: Springer-Verlag, 2003.

[12] W. M. Morrow, R. B. Paranjape, R. M. Rangayyan, and J. E. L. Desautels, "Region-based contrast enhancement of mammograms," *IEEE Trans. Med. Imag.*, vol. 11, pp. 392–406, 1992.